



Since January 2020 Elsevier has created a COVID-19 resource centre with free information in English and Mandarin on the novel coronavirus COVID-19. The COVID-19 resource centre is hosted on Elsevier Connect, the company's public news and information website.

Elsevier hereby grants permission to make all its COVID-19-related research that is available on the COVID-19 resource centre - including this research content - immediately available in PubMed Central and other publicly funded repositories, such as the WHO COVID database with rights for unrestricted research re-use and analyses in any form or by any means with acknowledgement of the original source. These permissions are granted for free by Elsevier for as long as the COVID-19 resource centre remains active.

Coronavirus Disease 2019 (COVID-19) CT Findings: A Systematic Review and Meta-analysis

SA-CME

Cuiping Bao, MD, PhD, Xuehuan Liu, MD, PhD, Han Zhang, BSC, Yiming Li, MD, PhD, Jun Liu, MD, PhD

Credits awarded for this enduring activity are designated "SA-CME" by the American Board of Radiology (ABR) and qualify toward fulfilling requirements for Maintenance of Certification (MOC) Part II: Lifelong Learning and Self-assessment. To access the SA-CME activity visit <https://cortex.acr.org/Presenters/CaseScript/CaseView?Info=W0WWdzqKpATzTc9ZuEaGA046Z9CWL%2bLiv0R9e8kpRvM%253d>. SA-CME credit for this article expires April 24, 2023.

Abstract

Purpose: To date, considerable knowledge gaps remain regarding the chest CT imaging features of coronavirus disease 2019 (COVID-19). We performed a systematic review and meta-analysis of results from published studies to date to provide a summary of evidence on detection of COVID-19 by chest CT and the expected CT imaging manifestations.

Methods: Studies were identified by searching PubMed database for articles published between December 2019 and February 2020. Pooled CT positive rate of COVID-19 and pooled incidence of CT imaging findings were estimated using a random-effect model.

Results: A total of 13 studies met inclusion criteria. The pooled positive rate of the CT imaging was 89.76% and 90.35% when only including thin-section chest CT. Typical CT signs were ground glass opacities (83.31%), ground glass opacities with mixed consolidation (58.42%), adjacent pleura thickening (52.46%), interlobular septal thickening (48.46%), and air bronchograms (46.46%). Other CT signs included crazy paving pattern (14.81%), pleural effusion (5.88%), bronchiectasis (5.42%), pericardial effusion (4.55%), and lymphadenopathy (3.38%). The most anatomic distributions were bilateral lung infection (78.2%) and peripheral distribution (76.95%). The incidences were highest in the right lower lobe (87.21%), left lower lobe (81.41%), and bilateral lower lobes (65.22%). The right upper lobe (65.22%), right middle lobe (54.95%), and left upper lobe (69.43%) were also commonly involved. The incidence of bilateral upper lobes was 60.87%. A considerable proportion of patients had three or more lobes involved (70.81%).

Conclusions: The detection of COVID-19 chest CT imaging is very high among symptomatic individuals at high risk, especially using thin-section chest CT. The most common CT features in patients affected by COVID-19 included ground glass opacities and consolidation involving the bilateral lungs in a peripheral distribution.

Key Words: CT imaging findings, COVID-19, ground glass opacities, meta-analysis, thin-section chest CT

J Am Coll Radiol 2020;17:701-709. Copyright © 2020 American College of Radiology

Department of Radiology, Tianjin Union Medical Center, Tianjin, China. Corresponding authors and reprints: Yiming Li, MD, PhD, Department of Radiology, Tianjin Union Medical Center, 190 Jieyuan Road, Hongqiao District, Tianjin 300121, PR China; e-mail: riminglee@126.com or Jun Liu, MD, PhD, Department of Radiology, Tianjin Union Medical Center, 190 Jieyuan Road, Hongqiao District, Tianjin 300121, PR China; e-mail: cjr.liujun@vip.163.com.

The authors state that they have no conflict of interest related to the material discussed in this article.

INTRODUCTION

Beginning in December 2019, a number of cases with pneumonia of unexplained cause occurred in Wuhan, Hubei province, China. Deep sequencing from lower respiratory tract samples confirmed infection was caused by a novel coronavirus that had previously not been found in humans or animals. Subsequently, this novel coronavirus was named coronavirus disease 2019 (COVID-19) by the World Health Organization [1]. COVID-19 infection causes clusters of severe respiratory illness, and its main

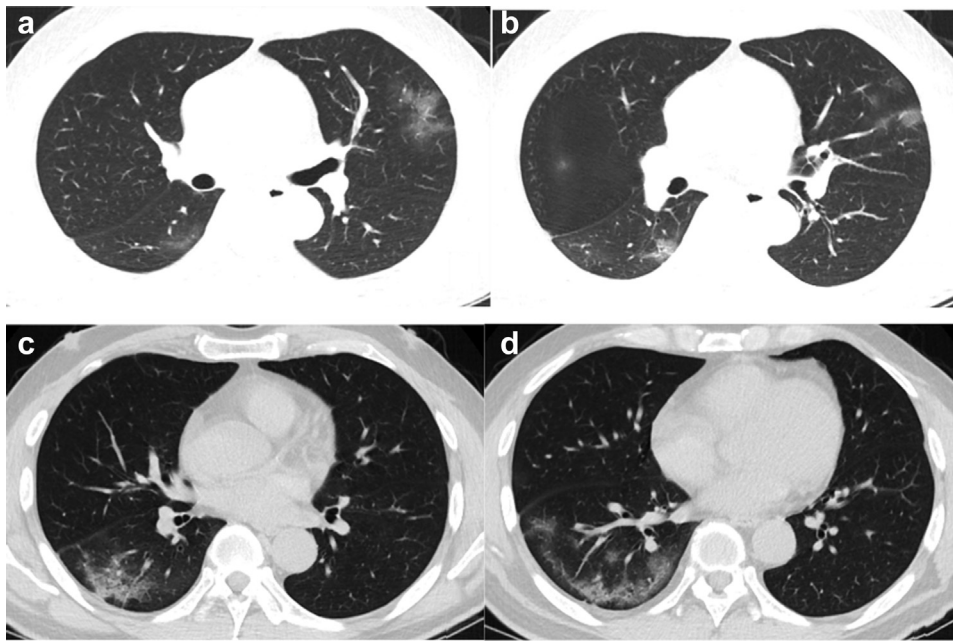


Fig 1. Baseline CT images (a-d) of a 50 year-old man admitted for symptoms of fever for 1 day: there were multiple patchy ground-glass opacities in the left upper lobe and right lower lobe (a, b). Air bronchogram and crazy paving pattern can be seen (c). Lesions are located in the peripheral area of the lung (d).

clinical manifestations are fever, cough, shortness of breath, and myalgia or fatigue [2,3]. Not only patients with symptoms but also patients in the incubation period can become the source of infection. Therefore, early diagnosis is very important.

Radiological examination, as a routine imaging tool for pneumonia diagnosis, is of great importance in the early detection and treatment of patients affected by COVID-19. Radiological examinations are relatively easy to perform and can produce fast diagnosis. Chest radiography is not sensitive

for the detection of ground-glass opacity (GGO) and may demonstrate normal findings in early stage of infection. In contrast, thin-section chest CT examination plays a key role in assisting diagnosis. To date, considerable knowledge gaps remain in the chest CT imaging features of COVID-19.

In this systematic review and meta-analysis, we aim to quantitatively summarize results from published studies to date to provide a more precise estimate of detection of COVID-19 by chest CT and report on the most common imaging findings on chest CT imaging.

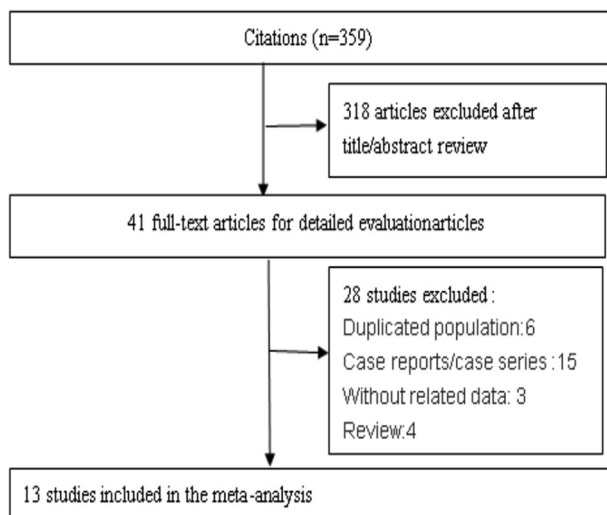


Fig 2. Flowchart on the article selection process.

MATERIALS AND METHODS

Retrieval of Studies

We searched PubMed for studies reporting CT imaging features of COVID-19 published between December 1, 2019, and February 29, 2020. The search terms included “COVID-19” OR “2019 Novel Coronavirus” OR “2019-nCoV”. In addition, we reviewed the reference lists of retrieved articles for additional articles. Two independent investigators screened titles or abstracts according to the inclusion and exclusion criteria. The meta-analysis was performed using Preferred Reporting Items for Systematic Reviews and Meta-Analyses guidelines.

Inclusion and Exclusion Criteria

Titles and abstracts of the articles were screened using the following inclusion criteria to identify all eligible studies: (1)

publications were original articles with full text; (2) the mean or median age of the study population was above 18 years; (3) at least one of the outcomes was chest CT imaging features of COVID-19; (4) the number of patients with corresponding imaging features was reported in the study. Studies were excluded if they (1) lacked corresponding outcome parameters or research data or (2) did not have available full texts. When there were multiple publications from the same population, only data from the most recent report or the study with the larger sample size was included.

Data Extraction

We extracted the following information from each publication: the first author's full name, study sample size, mean or median age, gender distribution, application of thin-section chest CT, results of chest CT imaging features, and number of patients with each corresponding imaging features. The recorded chest CT imaging features mainly included the following aspects: (1) patterns of the lesion (GGO, consolidation, GGO mixed consolidation, air bronchogram, interlobular septal thickening, crazy paving pattern, bronchiectasis, adjacent pleura thickening, pleural effusion, pericardial effusion, lymphadenopathy), (2) lesion distribution (bilateral lung, peripheral, central), and (3) lobe distribution and the number of lobes involved (Fig. 1).

Statistical Analysis

In this systematic review and meta-analysis, we pooled data using single-arm analysis. Because some proportions extracted from the original data were too high or too low, we transformed the data using the double arcsine method into a normal distribution. We conducted the meta-analysis using the transformed data. The pooled proportion was calculated using the result of the meta-analysis by the formula ($P = (\sin(tp/2))^2$). Statistical heterogeneity between studies was evaluated with Cochran's Q test and the I^2 statistic [4]. For the Q statistic, $P < .10$ was considered statistically significant for heterogeneity; for I^2 , a value $>50\%$ was considered to have severe heterogeneity. Publication bias was evaluated by constructing a funnel plot and by Egger's test [5]. For Egger's test, $P < .10$ was considered statistically significant. All statistical analyses were performed with Stata SE 12 (Stata Corp, College Station, TX) for Windows.

RESULTS

Characteristics of the Subjects in Selected Studies

Detailed search procedures are summarized in Figure 2. All of the full texts of the 41 identified articles were retrieved for

detailed evaluation. Of them, 28 articles did not meet the inclusion criteria, including 6 duplicated populations, 15 case reports or case series, 3 without related data, and 4 review articles. The remaining 13 independent studies were used in the current analysis [6-18] (Table 1). Of these studies, 10 studies reported one or more chest CT imaging signs [6-8,10-12,14-16,18], 11 studies reported at least one kind of lung distribution [6-8,10,11,13-18], and 5 studies reported the lobes and total number of lobes involved [7,9,11,15,16].

The 13 studies had 2,738 participants with 2,386 having abnormal CT imaging features. In the primary meta-analysis, we found that the pooled positive rate of the CT imaging was 89.76% (95% confidence interval [CI]: 84.42%-93.84%; Fig. 3). When we excluded the studies without mention of thin-section chest CT, the result was 90.35% (95%CI: 83.68%-95.42%).

Patterns of the Lesion

In this meta-analysis, we found that typical CT imaging appearance for COVID-19 patients was GGO. The incidence of GGO was 83.31% (95% CI: 69.43%-93.35%). When we excluded the studies without mention of thin-section chest CT, the incidence of GGO was 85.49% (95% CI: 64.74%-97.89%). The incidence of GGO with mixed consolidation was 58.42% (95% CI: 48.46%-67.58%; Fig. 4). The incidences of interlobular septal thickening, adjacent pleura thickening, and air bronchogram were also high: 48.46% (95% CI: 11.44%-86.19%), 52.46% (95% CI: 15.53%-87.54%), and 46.46% (95% CI: 17.76%-76.95%), respectively. The incidence of crazy paving pattern was 14.81% (95% CI: 6.61%-25.99%). Other atypical CT imaging findings included bronchiectasis (5.42%, 95% CI: 0.02%-19.31%), pleural effusion (5.88%, 95% CI: 3.38%-8.73%), pericardial effusion (4.55%, 95% CI: 2.09%-7.90%), and lymphadenopathy (3.38%, 95% CI: 1.00%-6.86%), respectively (Table 2).

Lesion Distribution

We found that most patients with COVID-19 have bilateral lung infection; the incidence was 78.2% (95% CI: 65.69%-88.19%). When we excluded the studies without mention of thin-section chest CT, bilateral lung infection was seen in 81.80% of patients (95% CI: 73.94%-88.51%). The lesions were mostly located in the peripheral area (76.95%, 95% CI: 57.43%-91.50%). Fewer lesions were located in the central (peribronchovascular) area (10.81%, 95% CI: 0.12%-41.50%; Table 2).

Table 1. Characteristics of 13 reviewed studies

| Study | Sample Size | Mean or Median Age | Gender | Thin-section Chest CT | CT Abnormal | CT Imaging Manifestations |
|--------------------|-------------|--------------------|--------------------------|-------------------------------|-------------|--|
| Zhang et al [18] | 9 | 35 | Male: 5 Female: 4 | Yes | 7 | GGO, consolidation, bilateral lung Pleural effusion |
| Song et al [11] | 51 | 49 | Male: 25 Female: 26 | Yes | 51 | GGO, consolidation, bilateral lung, peripheral, central, pleural effusion, pericardial effusion, lymphadenopathy |
| Pan et al [9] | 63 | 44.9 | Male: 33 Female: 30 | Yes | 63 | GGO, consolidation |
| Wu et al [14] | 80 | 44 | Male: 42 Female: 38 | Yes | 76 | GGO, consolidation, interlobular septal thickening, crazy paving pattern, pleural effusion, pericardial effusion, lymphadenopathy, peripheral, central |
| Bernheim et al [7] | 121 | 45.3 | Male: 61 Female: 60 | Yes (22 with conventional CT) | 94 | GGO, consolidation, crazy paving pattern, pleural effusion, bronchiectasis, lymphadenopathy, peripheral, central |
| Ai et al [6]. | 1,014 | 51 | Male: 467 Female: 547 | Yes | 888 | Bilateral lung, GGO, consolidation, interlobular septal thickening |
| Shi et al [10] | 81 | 49.5 | Male: 42 Female: 39 | Yes | 81 | Bilateral lung, GGO, consolidation, interlobular septal thickening, adjacent pleura thickening, air bronchogram, pleural effusion, bronchiectasis, lymphadenopathy, peripheral |
| Wang et al [12] | 52 | 44 | Male: 29 Female: 23 | Yes | 50 | GGO, consolidation, interlobular septal thickening |
| Xu et al [16] | 50 | 43.9 | Male: 29 Female: 21 | Yes | 41 | GGO, consolidation, interlobular septal thickening, air bronchogram, pleural effusion, peripheral, central |

(continued)

Table 1. Continued

| Study | Sample Size | Mean or Median Age | Gender | Thin-section Chest CT | CT Abnormal | CT Imaging Manifestations |
|------------------|--------------------------------|--------------------|--------------------------|-----------------------|-------------|--|
| Zhang et al [17] | 140 (135 with chest CT scan) | 57 | Male: 69 Female: 71 | Without mention | 134 | Bilateral lung |
| Guan et al [8] | 1,099 (975 with chest CT scan) | 47 | Male: 637 Female: 459 | Without mention | 840 | Bilateral lung, GGO, interlobular septal thickening, |
| Wu et al [13] | 80 | 46.1 | Male: 39 Female: 41 | Without mention | 55 | Bilateral lung |
| Xu et al [15] | 90 | 50 | Male: 39 Female: 51 | Yes | 69 | Bilateral lung, GGO, consolidation, crazy paving pattern, interlobular septal thickening, air bronchogram, adjacent pleura thickening, pleural effusion, pericardial effusion, lymphadenopathy, peripheral |

GGO = ground-glass opacities.

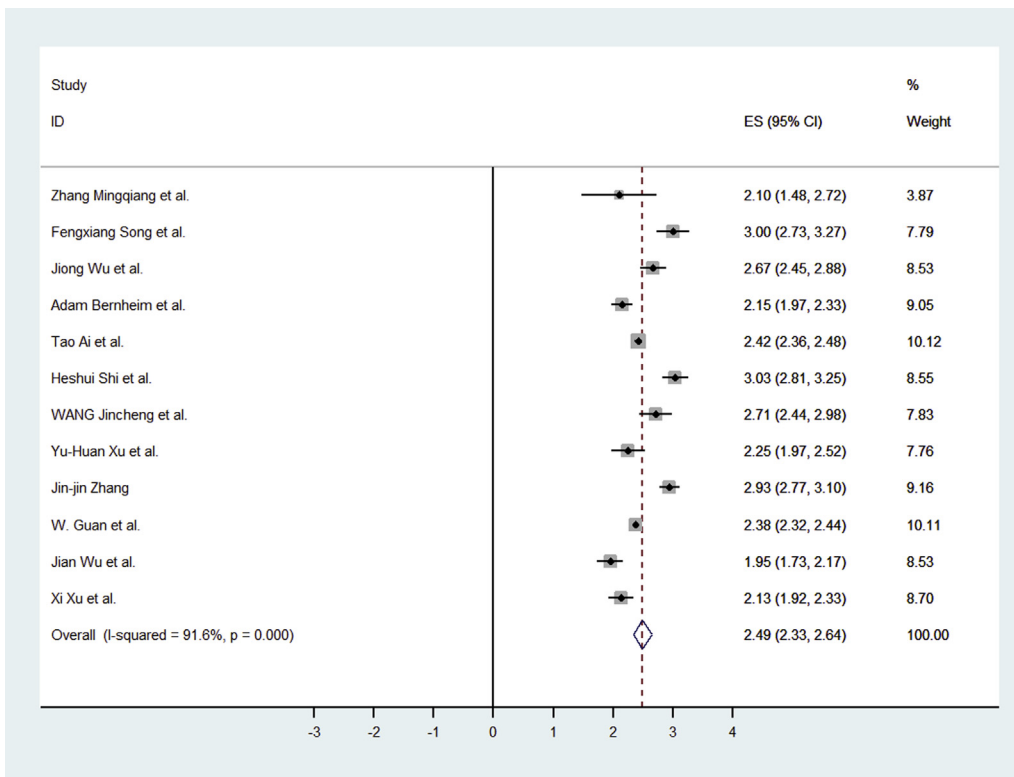


Fig 3. Forest plot of the studies for abnormal CT among presumed coronavirus disease 2019 infection. CI = confidence interval; ES = effect size.

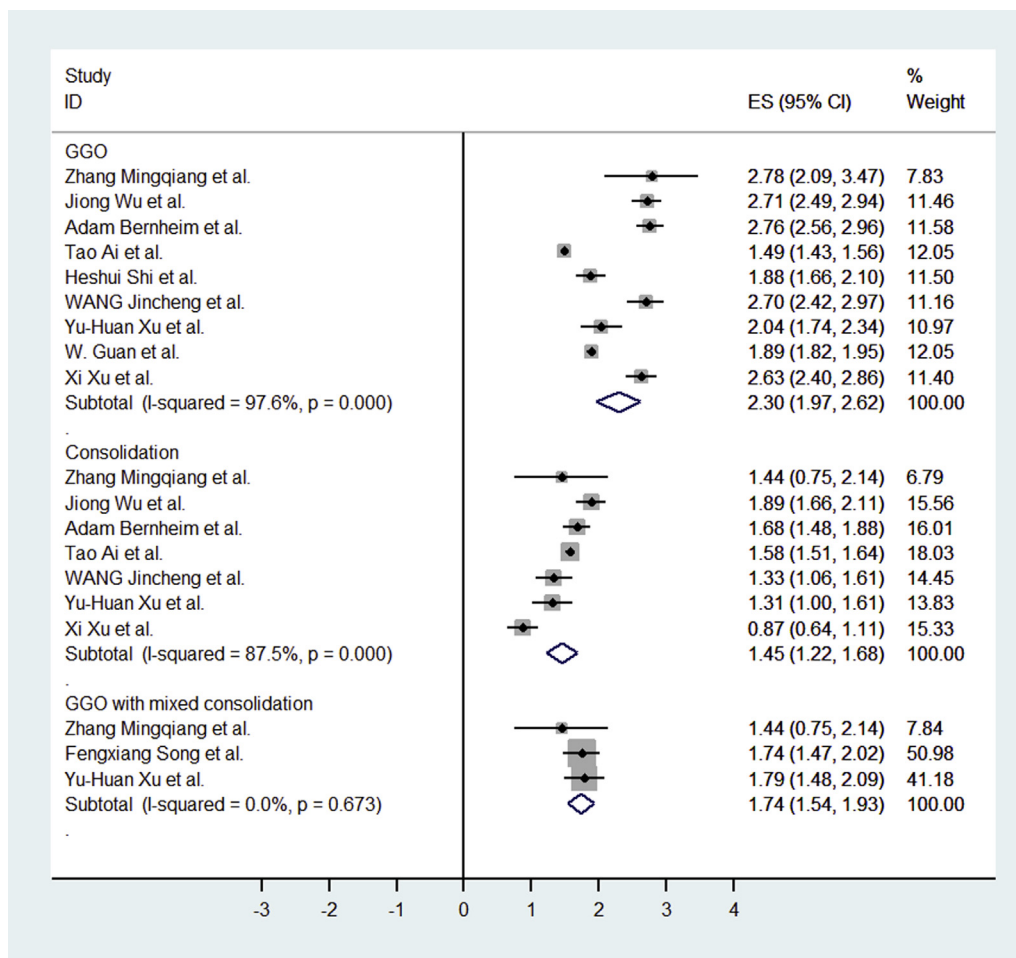


Fig 4. Forest plot of the studies for CT findings (GGO, consolidation, GGO with mixed consolidation). CI = confidence interval; ES = effect size; GGO = ground-glass opacities.

Lobe Distribution and Number of Lobes Involved

COVID-19 infection can involve all lobes. In this pooled meta-analysis, we found that the right lower lobe and left lower lobe were the most commonly involved; 87.21% (95% CI: 80.23%-92.84%) and 81.41% (95% CI: 76.1%-86.53%), respectively. The incidence of bilateral lower lobes was 65.22% (95% CI: 55.95%-73.94%). The right upper lobe and left upper lobe were also commonly involved: 65.22% (95% CI: 54.95%-75.24%) and 69.43% (95% CI: 58.91%-79.02%), respectively. The incidence of bilateral upper lobes was 60.87% (95% CI: 51.46-69.43%). More than half patients had right middle lobe infection (54.95%, 95% CI: 47.96%-61.36%). There were 39.54% (95% CI: 33.76%-45.96%) of patients with all lobes affected and 20.51% (95% CI: 13.76%-28.22%) patients with four lobes affected. A significant proportion of patients had three or more lobes involved (70.81%, 95% CI: 61.75%-79.10%; Table 2).

Publication Bias

P values for Egger's regression asymmetry test are shown in Table 3. There was a low probability of publication bias in the following subgroups: GGO mixed consolidation, air bronchogram, crazy paving pattern, pleural effusion, pericardial effusion, lymphadenopathy, peripheral, lobe of lesion distribution, and number of lobes involved. However, there was publication bias in the subgroup of abnormal GGO, consolidation, and bilateral lung involvement. Because there were only two studies in the subgroup of bronchiectasis, adjacent pleura thickening, central and bilateral upper lobes, and bilateral lower lobes, the publication bias could not be evaluated.

DISCUSSION

Our systematic review and meta-analysis suggests that the proportion of COVID-19 detected by chest CT imaging is very high. The most typical CT imaging finding is GGO.

Table 2. CT imaging findings in the meta-analysis

| CT Manifestations | Pooled Transformed Results (95% CI) | Pooled Proportion (95% CI)* |
|--------------------------------|-------------------------------------|-----------------------------|
| Patterns of the lesion | | |
| GGO | 2.3 (1.97-2.62) | 83.31 (69.43-93.35) |
| Consolidation | 1.45 (1.22-1.68) | 43.97 (32.82-55.45) |
| GGO mixed consolidation | 1.74 (1.54-1.93) | 58.42 (48.46-67.58) |
| Air bronchogram | 1.5 (0.87-2.14) | 46.46 (17.76-76.95) |
| Interlobular septal thickening | 1.54 (0.69-2.38) | 48.46 (11.44-86.19) |
| Crazy paving pattern | 0.79 (0.52-1.07) | 14.81 (6.61-25.99) |
| Bronchiectasis | 0.47 (0.03-0.91) | 5.42 (0.02-19.31) |
| Adjacent pleura thickening | 1.62 (0.81-2.42) | 52.46 (15.53-87.54) |
| Pleural effusion | 0.49 (0.37-0.6) | 5.88 (3.38-8.73) |
| Pericardial effusion | 0.43 (0.29-0.57) | 4.55 (2.09-7.90) |
| Lymphadenopathy | 0.37 (0.2-0.53) | 3.38 (1.00-6.86) |
| Lesion distribution | | |
| Bilateral lung | 2.17 (1.89-2.44) | 78.2 (65.69-88.19) |
| Peripheral | 2.14 (1.72-2.55) | 76.95 (57.43-91.50) |
| central | 0.67 (-0.07-1.4) | 10.81 (0.12-41.50) |
| Lobe of lesion distribution | | |
| Right upper lobe | 1.88 (1.67-2.1) | 65.22 (54.95-75.24) |
| Right middle lobe | 1.67 (1.53-1.8) | 54.95 (47.96-61.36) |
| Right lower lobe | 2.41 (2.22-2.6) | 87.21 (80.23-92.84) |
| Left upper lobe | 1.97 (1.75-2.19) | 69.43 (58.91-79.02) |
| Left lower lobe | 2.25 (2.12-2.39) | 81.41 (76.1-86.53) |
| Bilateral upper lobes | 1.79 (1.6-1.97) | 60.87 (51.46-69.43) |
| Bilateral lower lobes | 1.88 (1.69-2.07) | 65.22 (55.95-73.94) |
| Number of lobes involved | | |
| 1 | 0.81 (0.52-1.09) | 15.53 (6.61-26.88) |
| 2 | 0.75 (0.62-0.87) | 13.42 (9.31-17.76) |
| 3 | 0.67 (0.55-0.8) | 10.81 (7.37-15.16) |
| 4 | 0.94 (0.76-1.12) | 20.51 (13.76-28.22) |
| 5 | 1.36 (1.24-1.49) | 39.54 (33.76-45.96) |
| Lobes involved ≥ 3 | 2 (1.808-2.192) | 70.81 (61.75-79.10) |

CI = confidence interval; GGO = ground glass opacities.

*The results are expressed as a percentage.

Other common CT features in patients affected by COVID-19 included consolidation, interlobular septal thickening, adjacent pleura thickening, and air bronchograms. More than half of the patients manifested as GGO, consolidation, and adjacent pleura thickening. Imaging findings mostly involved the bilateral lungs and were located in the peripheral area of the lungs. The infection can involve all the lobes and mostly the bilateral lower lobes.

Some patients who had negative reverse-transcription polymerase chain reaction for COVID-19 at initial presentation may still show chest CT abnormalities [19]. Fang et al reported that the sensitivity of first reverse-transcription polymerase

chain reaction is 71%, which may be lower than that of chest CT [20]. In our meta-analysis of 2,738 cases, the pooled positive rate of CT imaging was 89.76% among patients suspected to have COVID-19. Thus, chest CT plays an important role in the early diagnosis of COVID-19.

In this analysis, we found that the typical CT features of COVID-19 are GGO and lung consolidation. Some of the GGO were further developed into reticular interlobular septa thickening and crazy paving pattern, indicating that the infection leads to diffuse alveolar edema and interstitial inflammation [21,22]. Several patients seemed to have pleural effusion, which may represent a poor prognostic

Table 3. Results of the Egger test

| CT Manifestations | P | Lobe of Lesion Distribution | P |
|--------------------------------|-------|-----------------------------|------|
| Abnormal CT | <.001 | Right upper lobe | .264 |
| GGO | .001 | Right middle lobe | .142 |
| Consolidation | .007 | Right lower lobe | .074 |
| GGO mixed consolidation | .116 | Left upper lobe | .056 |
| Air bronchogram | .974 | Left lower lobe | .064 |
| Interlobular septal thickening | .025 | Bilateral upper lobes | NA |
| Crazy paving pattern | .456 | Bilateral lower lobes | NA |
| Bronchiectasis | NA | Number of lobes involved | |
| Adjacent pleura thickening | NA | 1 | .379 |
| Pleural effusion | .675 | 2 | .189 |
| Pericardial effusion | .942 | 3 | .219 |
| Lymphadenopathy | .716 | 4 | .563 |
| Lesion distribution | | 5 | .067 |
| Bilateral lung | <.001 | Lobes involved ≥ 3 | .131 |
| Peripheral | .890 | | |
| Central | NA | | |

GGO = ground glass opacities; NA = the publication bias could not be tested.

indicator [23]. Generally, viral pneumonias have similar etiological mechanisms and typical imaging findings of COVID-19. Thus, these findings also appear in other viral pneumonia such as the common cold, influenza, and other coronavirus diseases including severe acute respiratory syndrome and Middle East respiratory syndrome [24-28].

Because COVID-19, severe acute respiratory syndrome, and Middle East respiratory syndrome all belong to the family of coronaviruses, the CT imaging signs are more similar. Still, there seems to be unique imaging characteristics for COVID-19. Unilateral involvement is more common in the early stage of severe acute respiratory syndrome and Middle East respiratory syndrome [29,30]. In contrast, COVID-19 infection seems to be more commonly bilateral. In this meta-analysis, most patients had bilateral lung involvement, especially the bilateral lower lobes. Overall, 70% of patients had three or more lobes involved.

Our meta-analysis has several strengths. First, the number of cases included was relatively large for 3 months of early publications, providing aggregate evidence for evaluating diagnosis of COVID-19 by chest CT. Second, the included studies were conducted in different hospitals and settings, making the results more generalizable. Third, in this analysis, we extract varieties of different imaging

features, including both specific imaging features and distribution patterns in the lungs.

Our meta-analysis also has several limitations. First, a majority of the studies included did not distinguish between clinically mild, moderate, and severe patients. Furthermore, some patients may have comorbidities and chronic diseases such as diabetes and hypertension that we cannot account for. These factors may affect imaging appearances. Second, because of different CT scanners and interpreting radiologists, the reported imaging features may be variable across sites.

TAKE-HOME POINTS

- Our systematic review and meta-analysis of the early literature suggests that the proportion of suspected COVID-19 detected by chest CT imaging is high.
- Chest CT, especially thin-section chest CT, can play a central role in early diagnosis of COVID-19.
- The most common CT features in patients affected by COVID-19 included GGO, consolidation, interlobular septal thickening, adjacent pleura thickening, and air bronchograms.
- The infection most commonly involves the bilateral lungs, especially bilateral lower lobes.

■ Similar imagine features are seen in other infections, and the final diagnosis of COVID-19 should still be based on reverse-transcription polymerase chain reaction.

REFERENCES

1. Nizzari M, Thellung S, Corsaro A, et al. Neurodegeneration in Alzheimer disease: role of amyloid precursor protein and presenilin 1 intracellular signaling. *J Toxicol* 2012;2012:187297.
2. Huang C, Wang Y, Li X, et al. Clinical features of patients infected with 2019 novel coronavirus in Wuhan, China. *Lancet* 2020;395:497-506.
3. Chen N, Zhou M, Dong X, et al. Epidemiological and clinical characteristics of 99 cases of 2019 novel coronavirus pneumonia in Wuhan, China: a descriptive study. *Lancet* 2020;395:507-13.
4. Higgins JP, Thompson SG. Quantifying heterogeneity in a meta-analysis. *Stat Med* 2002;21:1539-58.
5. Egger M, Davey Smith G, Schneider M, et al. Bias in meta-analysis detected by a simple, graphical test. *BMJ* 1997;315:629-34.
6. Ai T, Yang Z, Hou H, et al. Correlation of chest CT and RT-PCR testing in coronavirus disease 2019 (COVID-19) in China: a report of 1014 cases. *Radiology* 2020:200642.
7. Bernheim A, Mei X, Huang M, et al. Chest CT findings in coronavirus disease-19 (COVID-19): relationship to duration of infection. *Radiology* 2020:200463.
8. Guan WJ, Ni ZY, Hu Y, et al. Clinical characteristics of coronavirus disease 2019 in China. *N Engl J Med* 2020. Feb 28 [Online ahead of print].
9. Pan Y, Guan H, Zhou S, et al. Initial CT findings and temporal changes in patients with the novel coronavirus pneumonia (2019-nCoV): a study of 63 patients in Wuhan, China. *Eur Radiol* 2020. Feb 13 [Online ahead of print].
10. Shi H, Han X, Jiang N, et al. Radiological findings from 81 patients with COVID-19 pneumonia in Wuhan, China: a descriptive study. *Lancet Infect Dis* 2020;20:425-34.
11. Song F, Shi N, Shan F, et al. Emerging coronavirus 2019-nCoV pneumonia. *Radiology* 2020:200274.
12. Wang J, Liu J, Wang Y, et al. [Dynamic changes of chest CT imaging in patients with corona virus disease-19 (COVID-19)]. *Zhejiang Da Xue Xue Bao Yi Xue Ban* 2020;49: Feb 24 [Online ahead of print].
13. Wu J, Liu J, Zhao X, et al. Clinical characteristics of imported cases of COVID-19 in Jiangsu Province: a multicenter descriptive study. *Clin Infect Dis* 2020. Feb 29 [Online ahead of print].
14. Wu J, Wu X, Zeng W, et al. Chest CT Findings in patients with corona virus disease 2019 and its relationship with clinical features. *Invest Radiol* 2020;55:257-61.
15. Xu X, Yu C, Qu J, et al. Imaging and clinical features of patients with 2019 novel coronavirus SARS-CoV-2. *Eur J Nucl Med Mol Imaging* 2020;47:1275-80.
16. Xu YH, Dong JH, An WM, et al. Clinical and computed tomographic imaging features of novel coronavirus pneumonia caused by SARS-CoV-2. *J Infect* 2020;80:394-400.
17. Zhang JJ, Dong X, Cao YY, et al. Clinical characteristics of 140 patients infected with SARS-CoV-2 in Wuhan, China. *Allergy* 2020. Feb 19 [Online ahead of print].
18. Zhang MQ, Wang XH, Chen YL, et al. [Clinical features of 2019 novel coronavirus pneumonia in the early stage from a fever clinic in Beijing]. *Zhonghua Jie He He Hu Xi Za Zhi* 2020;43:E013.
19. Xie X, Zhong Z, Zhao W, et al. Chest CT for typical 2019-nCoV pneumonia: relationship to negative RT-PCR testing. *Radiology* 2020:200343.
20. Fang Y, Zhang H, Xie J, et al. Sensitivity of chest CT for COVID-19: comparison to RT-PCR. *Radiology* 2020:200432.
21. Chong S, Kim TS, Cho EY. Herpes simplex virus pneumonia: high-resolution CT findings. *Br J Radiol* 2010;83:585-9.
22. Wong KT, Antonio GE, Hui DS, et al. Thin-section CT of severe acute respiratory syndrome: evaluation of 73 patients exposed to or with the disease. *Radiology* 2003;228:395-400.
23. Das KM, Lee EY, Al Jawder SE, et al. Acute Middle East respiratory syndrome coronavirus: temporal lung changes observed on the chest radiographs of 55 patients. *AJR Am J Roentgenol* 2015;205:W267-74.
24. Malainou C, Herold S. [Influenza]. *Internist (Berl)* 2019;60:1127-35.
25. de Wit E, van Doremalen N, Falzarano D, et al. SARS and MERS: recent insights into emerging coronaviruses. *Nat Rev Microbiol* 2016;14:523-34.
26. Hui DSC, Zumla A. Severe acute respiratory syndrome: historical, epidemiologic, and clinical features. *Infect Dis Clin North Am* 2019;33:869-89.
27. Zu ZY, Jiang MD, Xu PP, et al. Coronavirus disease 2019 (COVID-19): a perspective from China. *Radiology* 2020:200490.
28. Kooraki S, Hosseiny M, Myers L, et al. Coronavirus (COVID-19) outbreak: what the department of radiology should know. *J Am Coll Radiol* 2020;17:447-51.
29. Ooi GC, Daqing M. SARS: radiological features. *Respirology* 2003;8(Suppl):S15-9.
30. Das KM, Lee EY, Langer RD, et al. Middle East respiratory syndrome coronavirus: what does a radiologist need to know? *AJR Am J Roentgenol* 2016;206:1193-201.